Advancing Early Cardiovascular Disease Prediction Model using Improved Beluga Whale Optimization with Ensemble Learning via ECG Signal Analytics

Hassan A. Alterazi[1,*]

[1]Department of Information Technology, Faculty of Computing and Information Technology, King Abdulaziz University, Jeddah, 21589, Saudi Arabia

Emails: haalterazi@kau.edu.sa

Abstract

Cardiovascular Disease (CVD) mainly affects the blood vessels and heart such as coronary artery disease, stroke, and heart failure. Early recognition is vital for on-time intervention and enhanced patient results. CVD is a major issue in society nowadays. When compared to the non-invasive model, the electrocardiogram (ECG) is the most effective approach for identifying cardiac defects. However, ECG analysis needs an experienced person with high knowledge and basically, it is a time-consuming task. Emerging a new technique to identify the disease at an early stage increases the quality and efficacy of medicinal care. A state-of-the-art technologies like machine learning (ML) and artificial intelligence (AI) have been gradually being used to increase the efficacy and accuracy of CVD recognition, permitting for faster and more exact analysis, and finally contributing to superior management and prevention tactics for CV health. This research paper designs an Early Cardiovascular Disease Prediction using an Improved Beluga Whale Optimizer with Ensemble Learning (ECVDP-IBWOEL) approach via ECG Signal Analytics. The main intention of the ECVDP-IBWOEL system is to forecast the presence of CVD at the early stage using EEG signals. In the ECVDP-IBWOEL method, the primary phase of data preprocessing is initially implemented to convert the input data into a well-suited layout. Also, the ECVDP-IBWOEL technique follows an ensemble learning (EL) process for CVD detection comprising three models namely long short-term memory (LSTM), deep belief networks (DBNs), and stacked autoencoder (SAE). Finally, the IBWO algorithm-based hyperparameter tuning process takes place which can boost the classifier results of the ensemble models. To certify the enhanced results of the ECVDP-IBWOEL system, an extensive experimental study is made. The experimentation outcomes stated that the ECVDP-IBWOEL system underlines promising performance in the CVD prediction process

Keywords: Cardiovascular Disease; Electrocardiogram; Ensemble Learning; Beluga Whale Optimization; Data Preprocessing

1. Introduction

Cardiovascular disease (CVD) is a dangerous health issue that affects numerous persons worldwide and is a foremost cause of death as well [1]. The lost efficiency, cost of healthcare, and reduced life quality owing to heart disease have a major financial and social effect on persons, family members, and society. This highlights the value of initial disease classification [2]. Where the electrocardiogram (ECG) is considered a highly critical technique for identifying and analyzing cardiac issues. However, the ECG captures time and needs skilled experts with specialized knowledge to understand about it [3]. Also, numerous devices are accessible that can record signals of ECG and grow greatly. The ECG is a significant medical device that records the features of cardiac transmission, retrieval, and excitatory for automatic recognition of CVD [4]. It is essential to identify the uneven heartbeats existing in the ECG signal. For clarification of the ECG, recording physical inspection is vital but it is tedious and time-consuming [5]. The feature extractor is one of the difficulties in analyzing ECG. Present classification

DOI: https://doi.org/10.54216/FPA.170213
Received: January 28, 2024 Revised: April 27, 2024 Accepted: September 26, 2024

methods remove medical features by signal processing means. To categorize the ECG, methods incorporate the features and equate them with features removed on numerous heart illnesses [6]. Nevertheless, owing to noise restriction, few features were complex to remove.

The most important modules for the discovery and resolution of CVD diseases are the extraction and identification of beats [7]. For instance, several persons endure the negative effects of heartbeats, which is final in a few cases. As an outcome, it is extremely necessary to precisely and reasonably identify hypertrophic heart rate [8]. The value of visual characterization of the ECG signals and the features attained are certain aspects of ECG frame identification. The heart rate classification has currently been estimated by many experts using a collection of features that state many techniques of ECG classification. The heart rate features include ECG syllables, heart rate breaks, beats, and harmonics at peak recognition. The identification procedure aims to gain a clever method, that is efficient of categorizing any heart rate, and signal to an exact kind of heart rate [9]. CVD has dissimilar features, which it is impossible to project a method that can remove all the mandatory features. This creates every diagnostic method with low accuracy and poor scalability. Presently, the deep learning (DL) model has developed as a great solution for ECG analysis. Deep convolutional neural networks (CNNs) remove features mechanically from the original images or signals [10]. Owing to its great performance in automatic classification, DNNs-based ECG analysis has become gradually promising.

This paper develops an Early Cardiovascular Disease Prediction employing Improved Beluga Whale Optimization with Ensemble Learning (ECVDP-IBWOEL) technique via ECG Signal Analytics. In the ECVDP-IBWOEL system, the primary phase of data preprocessing is initially performed to convert the input dataset into the well-suited format. Besides, the ECVDP-IBWOEL technique follows the EL process for CVD detection comprising three models namely long short term memory (LSTM), deep belief networks (DBNs), and stacked auto encoder (SAE). Finally, the IBWO algorithm-based hyperparameter tuning process takes place which can boost the classifier results of the ensemble models. The experimental outcome stated that the ECVDP-IBWOEL algorithm underlines optimistic performance in the CVD prediction process.

2. Literature Works

Zhang et al. [11] proposed a CPDNet for endwise CVD recognition. Specifically, a new progressive dense fusion tactic is planned. While, the approach combined region-aware, cross-modality, and multi-scale feature optimizer modules. Furthermore, a new co-learning tactic is intended to direct the learning procedure of the CPDNet by merging intra modality and common damages. Karthik et al. [12] projects an automatic DL-based 1D biomedical ECG-CVD technique. Once the pre-processing is done, a DBNs method is employed in order to originate a feature vector. Also, an ISSO model has been utilized for the hyperparameter tuning. Finally, the XGBoost model is used to assign appropriate class labels. In [13], a new enhanced framework termed as WbGAS method was intended for forecasting and identifying heart illness utilizing the ECG dataset. The composed database has 3 classes, which is prepared and trained utilizing the projected WbGAS model.

In [14], a new technique is planned dependent upon the attention-based DL method. A 1D-CNN is utilized for extraction and the HOS feature from the raw signals. The weight has been altered with the suggested ARR-LO. At last, the combined features are sustained into the hybrid attention method over the DTCN and LSTM, where ARR-LO is employed. Golande and Pavankumar [15] main aim is to improve the ECG-based heart illness identification efficacy by utilizing a hybrid feature engineering technique. This approach projects a hybrid model utilizing a conventional ECG beats extractor system and CNN-based feature. For the prediction of heart disease, the feature vector has been maintained consecutively in the DL classifier LSTM model.

Rai et al. [16] projected a successive ensemble model by executing a hybrid data re-sampling method named “SMOTE and Tomek Link (SMOTE + Tomek)". The successive ensemble model uses dual different DL methods namely CNNs and a hybrid model, CNN-LSTM method. In [17], an innovative technique based on DL is developed. The developed model is based on 3 main modules namely BI-LSTM layer, inception-ResNet structure, and a multi-scale signal analysis method. This approach proposed a 3-phase CBD filter that consecutively includes Daubechies, Butterworth, and Chebyshev filters. This technique also joined this filter with the DL and multi-scale models. Tahmid et al. [18] developed an MD-CardioNet, an effective DL structure by employing multi-dimensional (1D, 2D, and 3D) convolutions. Sequential feature extractors take time-dependent data, but a two-dimensional convolutional is used to create an image sign from the multichannel ECG signals and removes inter-channel feature. In order to decrease computational difficulty, a real knowledge distillation structure is presented.

DOI: https://doi.org/10.54216/FPA.170213
Received: January 28, 2024 Revised: April 27, 2024 Accepted: September 26, 2024

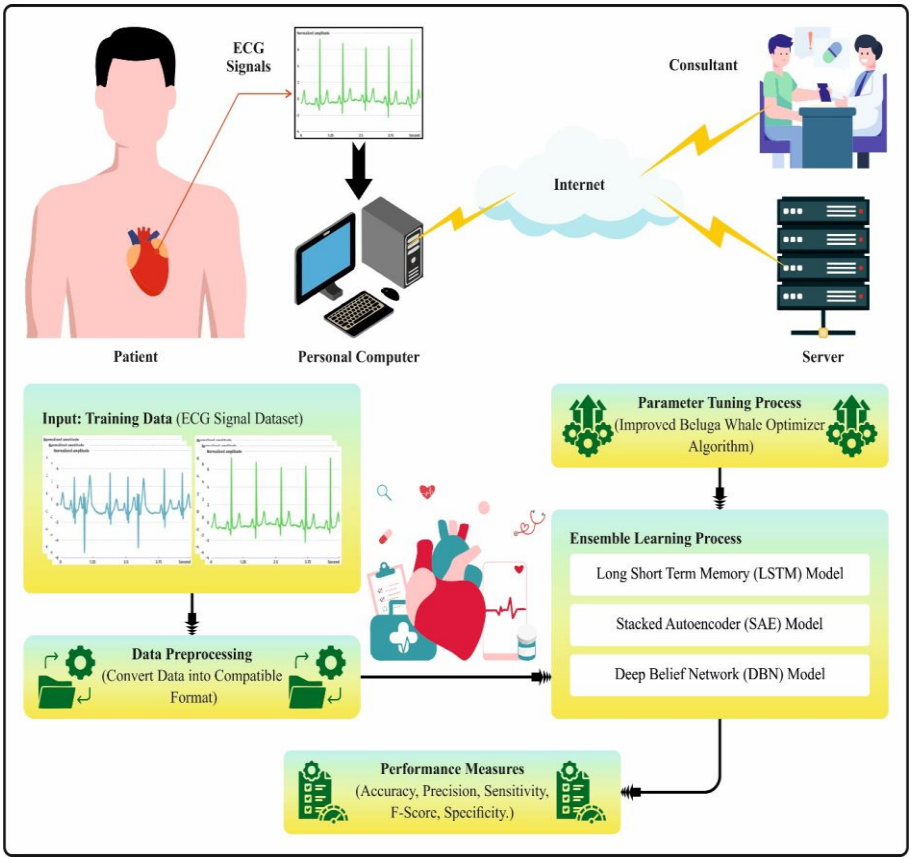

Figure 1. Workflow of ECVDP-IBWOEL technique

3. The Proposed Method

In this work, we have developed an ECVDP-IBWOEL technique via ECG signal analytics. The key purpose of the ECVDP-IBWOEL algorithm is to forecast the presence of CVD at the early stage using EEG signals. To accomplish that, the ECVDP-IBWOEL technique has three different kinds of methods such as data pre-processing, ensemble learning, and IBWO-based hyperparameter tuning procedure. Fig. 1 represents the work flow of the ECVDP-IBWOEL model.

A. Data Preprocessing

Initially, the ECVDP-IBWOEL technique arises data preprocessing is performed to transform the input dataset into the compatible layout. During the stage of data pre-processing, a cluster of 3000 ECG signals has been employed for experimentation research. Whereas, the cluster of 35 ECG signals enclosed NULL as classes, so it must be extracted. Also, the residual 2965 should be employed for the experiment. Also, a sample rate of 100 has been nominated from the dual sample rates of 100 and 500 in the dataset.

B. Ensemble Learning

The ECVDP-IBWOEL technique follows the EL process for CVD detection including three models such as LSTM, DBN, and SAE.

i) LSTM Model

In the sequential data, RNNs can be the ability to model dynamic temporal dependencies employing internal description of prior conditions and existing inputs [19]. This behavior permits RNNs to forecast the future statuses of a time sequence by demonstrating them as an operation of preceding layers. The RNN output in time-step t will be calculated as:

$$h[t] = \tanh(W_{ii}x[t] + b_{ii} + W_{hi}h[t-1] + b_{hi}) \quad (1)$$

$$o[t] = \tanh(W_{oh}h[t] + b_{oh}) \quad (2)$$

DOI: https://doi.org/10.54216/FPA.170213
Received: January 28, 2024 Revised: April 27, 2024 Accepted: September 26, 2024

Now, $h[t]$ and $x[t]$ describes the existing hidden and input vectors, and $h[t-1]$ defines the hidden layer (HL) at the preceding time step. In the presented in Eq. (1), the HL in time-step t is measured as a total weight of earlier HL $h[t-1]$ and $x[t]$. The weights for such calculation have been specified by W_i, and bias b_h. Lastly, the output $\mathrm{o}[t]$ can be calculated as a biased summation of the HL at time step t, as presented in Eq. 5. W_o denotes the weight and b_o is the bias.

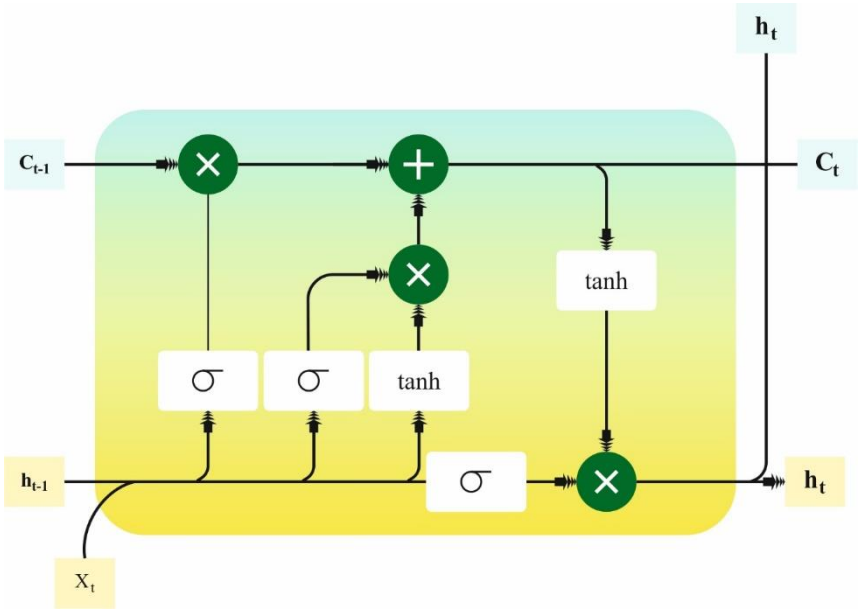

Figure 2. Architecture of LSTM

Regardless of their great efficiency, RNN tends to be impacted from the challenges of vanishing gradients which employed for backpropagation (BP) reduces rapidly in various HL. For this reason RNNs get lesser valuable while it derives to learn comparatively extended temporal dependencies. LSTM deals with this complexity by separating every component into numerous gates. A traditional LSTM unit comprises a cell status, input gate, forget gate, and output gate. The cell status will be accountable to store data through random time intervals. Fig. 2 depicts the structure of LSTM. The LSTM input at time-step t will be managed by applying these gates and formulations are given below:

$$i[t] = \sigma(W_{ii}x[t] + b_{ii} + W_{ih}h[t-1] + b_{ih}) \quad (3)$$

$$f[t] = \sigma\big(W_{fi}x[t] + b_{fi} + W_{fh}h[t-1] + b_{fh}\big) \quad (4)$$

$$\mathrm{o}[t] = \sigma(W_{oi}x[t] + b_{oi} + W_{oh}h[t-1] + b_{oh}) \quad (5)$$

$$C[t] = tanh(W_{oi}x[t] + b_{oi} + W_{oh}h[t-1] + b_{oh}) \quad (6)$$

Now, $x[t]$ refers to the existing input state and $h[t]$ defines the existing HL that also executes the output for the LSTM model. These gates have been denoted by $f[t]$, $i[t]$, and $\mathrm{o}[t]$, correspondingly. The output will be employed for updating the memory and hidden statuses at time-step t as:

$$c[t] = f[t] \odot c[t-1] + i[t] \odot \hat{c}[t] \quad (7)$$

$$h[t] = \mathrm{o}[t] \odot \tanh\,(c[t]) \quad (8)$$

whereas $c[t]$ indicates the cell state and $\hat{c}[t]$ denotes the candidate or memory state.

From the Eq. (3) the input gate employs distinct weights and bias $\{W_{ii}, b_{ii}\}$ and $\{W_{ih}, b_{ih}\}$ for the inputs x_t and prior HL h_{t-1}, correspondingly. The forget gate from Eq. (4) and output gate from Eq. (5) equally calculate a linear integration and HL with an activation function of sigmoid. While the candidate status (Eq. (6)) can be calculated as the functions of HL and input state. Then, the cell status is measured by the addition of matrix dot products of $f[t]$ and $c[t-1]$ to the matrix dot products of $i[t]$ and $C[t]$. The applied hyperbolic tangent function $(tanh)$ rather than the sigmoid. Lastly, the hidden state has been calculated by taking the hyperbolic tan of $c[t]$ and the matrix dot product of $\mathrm{o}[t]$.

DOI: https://doi.org/10.54216/FPA.170213
Received: January 28, 2024 Revised: April 27, 2024 Accepted: September 26, 2024

ii) DBN Model

DBNs is a DL technique dependent upon data probability distribution. DBN contains of manifold-restricted Boltzmann machine (RBM) and a BP [20]. RBM is the essential unit of DBN that executes data mining and feature extractor. An RBM is a dual-layer NN that contains a VL and a HL. There is no link among RBM modules in the similar layer, and no data contacts have been implemented. By the weights, the layers are linked to everyone. The VL is employed to input data, and entire nodes in the HL capture randomly generated values of 0 or 1. In the RBM layer, there is no link relation; so, the conditions of the modules are autonomous of everyone and upgraded in equivalent. Thus, it is very simple to get the probability distribution of the HL and VL. When the input signal is formed, the possibility of the HL module being initiated has been exposed in Eq. (9):

$$P(h=1|v,\theta)=\prod_{j=0}^{m}\frac{1}{\left(1+\exp\left(-W_j^T v-b_j\right)\right)} \tag{9}$$

If the HL node is formed, the probability of the VL reform module being initiated is presented in Eq. (10):

$$P(v=1|h,\theta)=\prod_{i=0}^{m}\frac{1}{\left(1+\exp(-W_i^T h-a_i)\right)} \tag{10}$$

RBM employs the model of reducing the contrastive divergence (MCD) for its training method to attain the reason of diminishing the error among the rebuilt signals of the VL and the new signal. So, below the RBM alteration of the momentum m and learning rate η, the upgrade rule is displayed in Eq. (11):

$$\begin{cases} W_{n+1}\leftarrow m_n^W+\eta(\langle v_i h_j\rangle_{data}-\langle v_i h_j\rangle_{model}) \\ a_{n+1}\leftarrow m_n^a+\eta(\langle v_i\rangle_{data}-\langle v_i\rangle_{model}) \\ b_{n+1}\leftarrow m_n^b+\eta(\langle h_i\rangle_{data}-\langle h_i\rangle_{model}) \end{cases} \tag{11}$$

Here, m denotes momentum, η signifies the learning rate, $\langle\cdot\rangle_{data}$ indicates $P(h|v,\theta)$, and $\langle\cdot\rangle_{model}$ denotes $P(v|h,\theta)$. The DBN model training contains dual procedures namely unsupervised and supervised learning. During the unsupervised learning stage, the DBNs trust on RBM to utilize greedy models to implement deep mining and feature learning of input data. In the phase of supervised learning, the DBNs are considered as a BP neural networks which are set with limitations. As per to the error among the learning method and the real outcomes, the model limits have been additionally modified to finish the training. The unsupervised learning defeats the sensitivity of the classical neural network of BP to early parameters and enhances the efficacy of convergence and learning in the phase of supervised training model.

iii) SAE Model

AE is the fundamental module of a SAE composition and task. Generally, the AE is a 3-layer neural networks containing an HL, an output layer and visible layer (VL). An AE is divided into dual parts namely a decoder and an encoder. SAE is a DL method collected of numerous AEs, whereas the output of every HL is linked to the input of the following HL. Once, all HL are trained, a BP model has been utilized to minimalize the price and upgrade the weights by a labeled training set for succeeding modification. During the encoding, the mapping of higher-dimensional information from the input to the HL is the data fusion and feature learning.

$$y=sigmoid(Wx+b) \tag{12}$$

Here, x denotes the input data; b signifies the offset vector; and W denotes the weight matrix.

At the decode part, the mapping from HL to output layer has been considered as reinstating the learned deep feature data to the new one.

$$y=sigmoid(W'h+b') \tag{13}$$

Whereas b' signifies the offset vector, h denotes the learned deep feature data and W' states the weight matrix. Then, the output and input structure are similar, the AE training method is a self-supervised learning procedure. Constantly decreasing the error among the output and input data recognizes the AE training. This paper utilizes the cost function of mean square error as an extent of model training, which definite as follows:

DOI: https://doi.org/10.54216/FPA.170213
Received: January 28, 2024 Revised: April 27, 2024 Accepted: September 26, 2024

$$E = \frac{1}{S}\sum_{j=1}^{S}\frac{1}{2}\sum_{i=1}^{n}\left(x_i^j - y_i^j\right)^2 \tag{14}$$

C. Hyperparameter Tuning using IBWO Model

Finally, the IBWO algorithm-based hyperparameter tuning process takes place which has the ability to boost the classifier results of the ensemble models. The BWO model was stimulated by the beluga whale's behavior such as feeding, swimming, and whale falling [21]. This technique contains 3 phases such as exploration, growth and a whale falling. In the optimizer procedure, the whale fall stage has been executed at the end of every iteration of the mining and exploration stages. The stages of white whale optimizer (WWO) method are mentioned below.

Step 1: Initialize

Define the parameters that contains the populace size and the highest iteration count $T_{\max}$. Create the first locations of belugas in the searching space randomly.

Step 2: Phase of Exploitation and Exploration

Based on the factor of balancing B_f, every beluga selects where to join either in exploration or exploitation stage. If $B_f > 0.5$, the whale picks the exploration stage which is restored by Eq. (15).

$$\begin{Bmatrix} X_{i,j}^{T+1} = X_{i,Pj}^{T} + \left(X_{r,P_1}^{T} - X_{i,Pj}^{T}\right)\cdot(1+r_1)sinl2\pi r_2), j = even \\ X_{i,j}^{T+1} = X_{i,Pj}^{T} + \left(X_{r,P_1}^{T} - X_{i,Pj}^{T}\right)\cdot(1+r_1)\cos(2\pi r_2), j = odd \end{Bmatrix} \tag{15}$$

Here, $X_{i,j}^{T+1}$ denotes novel position, p_j refers the random number, $X_{i,Pj}^{T}$ signifies the location of the i^{th}beluga whale on p_j dimension, $X_{i,Pj}^{T} and X_{r,P_1}^{T}$ represents the present locations for ith and r represents the arbitrarily chosen beluga whale, r_1 and r_2 denotes the randomly generated number among $(0,1)$. The random numbers of r_1 and r_2 are employed to improve the arbitrary operators in the stage of exploration. If $B_f < 0.5$, then it arrives at the exploitation stage that upgraded utilizing Eq. (16). Then, the novel position fitness value has been intended and placed to discover the finest outcome in the existing iteration.

$$X_i^{T+1} = r_3\cdot X_{best}^{T} - r_4\cdot X_i^{T} + 2r_4\cdot\left(1 - \frac{T}{T_{\max}}\right)\cdot L_F\cdot\left(X_r^{T} - X_i^{T}\right) \tag{16}$$

Whereas, X_i^T and X_r^T denote the existing location for the ith and a arbitrary beluga whale,

X_i^{T+1} specifies the novel location of the ith beluga whale, X_{best}^{T} refers to the best location between beluga whales, r_3 and r_4 are the randomly produced numbers $(0,1)$. L_F states the Levy flight function and expressed as:

$$L_F = 0.05\cdot\frac{u\cdot\sigma}{|v|^{\frac{1}{\beta}}} \tag{17}$$

$$\sigma = \left(\frac{\Gamma\cdot(1+\beta)\cdot\sin\left(\frac{\pi\beta}{2}\right)}{\Gamma\cdot\left(\frac{1+\beta}{2}\right)\cdot\beta\cdot 2^{\frac{\beta-1}{2}}}\right) \tag{18}$$

Here, u and v are randomly generated numbers and β is 1.5.

Step 3: Whale fall stage

Few belugas might perish and drop into the sea. Where the possibility of a whale subsiding is intended at every iteration W_f. So, the position of the belugas is upgraded as per Eq. (19).

$$X_i^{T+1} = r_5\cdot X_i^{T} - r_6\cdot X_r^{T} + r_7\cdot X_{step} \tag{19}$$

Whereas r_5, r_6, and r_7 are randomly generated values among $(0,1)$, X_{step} denotes the step size. The equation is expressed below:

$$X_{step} = (u_b - l_b)\cdot\exp\left(-2W_f\cdot n\cdot\frac{T}{T_{\max}}\right) \tag{20}$$

The probability of a whale falling has been projected utilizing this method as a linear function:

DOI: https://doi.org/10.54216/FPA.170213
Received: January 28, 2024 Revised: April 27, 2024 Accepted: September 26, 2024

$$W_f = 0.1 - 0.05 \cdot \frac{T}{T_{\max}} \tag{21}$$

The author looks onward to the growth of the BWO multi-objective optimizer model. Inadequate populace variability and spatial exploration ability are the main problems that are given to local optimal. In this study paper, these problems are addressed. The overview of the logistic chaotic map and the dissimilarity variant operator improves the whole performance of algorithms. Also, to enlarge the search step, in Eq. (17), the co-efficient of 0.05 is changed to 1 in this paper.

To enhance the populace variability and deliver the initial candidate solution, chaotic mapping was used. Also, to improve search skills, chaotic mapping helps optimizer methods positively in order to prevent local optimal solutions. Dual general mapping models such as Logistic and Tent mapping are employed for defining the beginning points of optimizer models and make initial values. Logistic mapping is defined in Eq. (22):

$$x \cdot (k+1) = \mu \cdot x(k) \cdot \big(1 - x(k)\big) \tag{22}$$

Whereas, $x(k) \in (0,1)$ and $3.5699 < \mu \leq 4$, the method is in chaos. If μ is near 4, the chaotic sequence is generated uniformly among 0 and 1 as nonperiodic and nonconverging. So, the μ parameter must be set near to 4. Logistic map was applied to attain the $x_{ij}(k+1)$ by Eq. (23).

$$x_{ij} \cdot (k+1) = 4 \cdot x_{ij}(k) \cdot \Big(1 - x_{ij}(k)\Big) \tag{23}$$

Where, by calculation, $x_{ij}(k+1)$ is changed from the original domain of [0,1] to a novel x_{ij} as per Eq. (24), where lb and ub denote the lower and upper bound of x_{ij}, respectively.

$$x_{ij} = lb + x_{ij} \cdot (k+1) \cdot (ub - lb) \tag{24}$$

The IBWO model improves a fitness function (FF) to accomplish amplified classifier performance. It defines a positive number to represent the greater candidate solution performance. In this research, the classifier rate of error minimization is reflected as FF, which is certain in Eq. (25).

$$fitness(x_i) = ClassifierErrorRate(x_i)$$
$$= \frac{No.of\ misclassified\ samples}{Total\ no.of\ samples} * 100 \tag{25}$$

4. Result Analysis and Discussion

The simulation analysis of the ECVDP-IBWOEL algorithm was verified on the PTB-XL dataset [22]. The database has five classes namely Hypertrophy (HYP), Conduction Disturbance (CD), Myocardial Infarction (MI), ST/T Change (STTC), and Normal ECG (NORM). In Table 1 and Fig. 3, the CVD predictive results of the ECVDP-IBWOEL model are clearly stated under distinct number of epochs. The outcomes highlighted that the ECVDP-IBWOEL system obtains efficient outcomes under all epochs.

Table 1: CVD predictive outcome of ECVDP-IBWOEL technique under various epochs

500 EPOCH					
Measures	$Sens_y$	$Spec_y$	$Accu_y$	$Prec_n$	F_{Score}
CD	98.90	57.92	91.20	90.27	94.57
HYP	98.70	66.16	99.89	96.88	98.02
MI	97.69	51.05	94.89	88.20	94.56
NORM	73.01	82.31	82.87	80.21	73.77
STTC	95.84	53.10	92.11	87.41	93.21
Average	92.83	62.11	92.19	88.59	90.82
1000 EPOCH					
Measures	$Sens_y$	$Spec_y$	$Accu_y$	$Prec_n$	F_{Score}
CD	98.78	57.22	93.61	89.25	94.13
HYP	99.52	59.83	96.88	93.22	97.42

DOI: https://doi.org/10.54216/FPA.170213
Received: January 28, 2024 Revised: April 27, 2024 Accepted: September 26, 2024

MI	98.04	46.45	91.80	89.10	93.72
NORM	72.07	83.52	80.14	79.85	74.07
STTC	95.49	52.46	90.90	87.63	90.67
Average	92.78	59.90	90.67	87.81	90.00
1500 EPOCH					
Measures	$Sens_y$	$Spec_y$	$Accu_y$	$Prec_n$	F_{Score}
CD	97.82	58.34	94.03	88.50	92.94
HYP	97.99	61.25	98.09	94.81	95.78
MI	98.34	50.41	94.28	90.67	92.71
NORM	71.52	84.63	81.64	78.63	75.69
STTC	96.88	54.80	90.43	86.13	91.35
Average	92.51	61.89	91.69	87.75	89.69
2000 EPOCH					
Measures	$Sens_y$	$Spec_y$	$Accu_y$	$Prec_n$	F_{Score}
CD	97.53	59.10	95.22	90.28	92.56
HYP	98.44	60.29	97.08	95.85	96.06
MI	99.00	50.13	92.31	89.05	92.38
NORM	72.15	83.06	83.72	78.16	74.89
STTC	96.29	55.32	93.07	86.71	91.55
Average	92.68	61.58	92.28	88.01	89.49

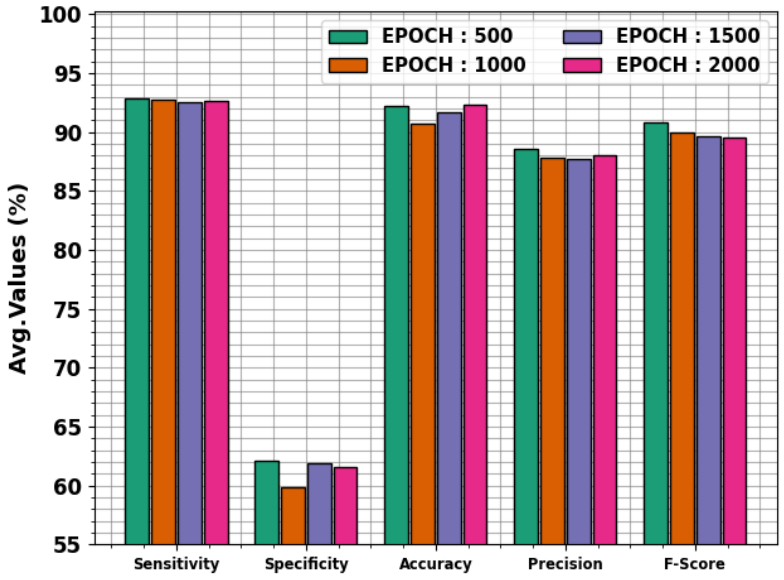

Figure 3. Average outcome of ECVDP-IBWOEL technique under distinct epochs

With 500 epochs, the ECVDP-IBWOEL technique achieves an average $sens_y$ of 92.83%, $spec_y$ of 62.11%, $accu_y$ of 92.19%, $prec_n$ of 88.59%, and F_{score} of 90.82%. Along with that, with 1000 epochs, the ECVDP-IBWOEL model gets an average $sens_y$ of 92.78%, $spec_y$ of 59.90%, $accu_y$ of 90.67%, $prec_n$ of 87.81%, and F_{score} of 90%. Also, with 1500 epochs, the ECVDP-IBWOEL method attains an average $sens_y$ of 92.51%, $spec_y$ of 61.89%, $accu_y$ of 91.69%, $prec_n$ of 87.75%, and F_{score} of 89.69%. Furthermore, with 2000 epochs, the ECVDP-IBWOEL approach acquires an average $sens_y$ of 92.68%, $spec_y$ of 61.58%, $accu_y$ of 92.28%, $prec_n$ of 88.01%, and F_{score} of 89.49%.

DOI: https://doi.org/10.54216/FPA.170213
Received: January 28, 2024 Revised: April 27, 2024 Accepted: September 26, 2024

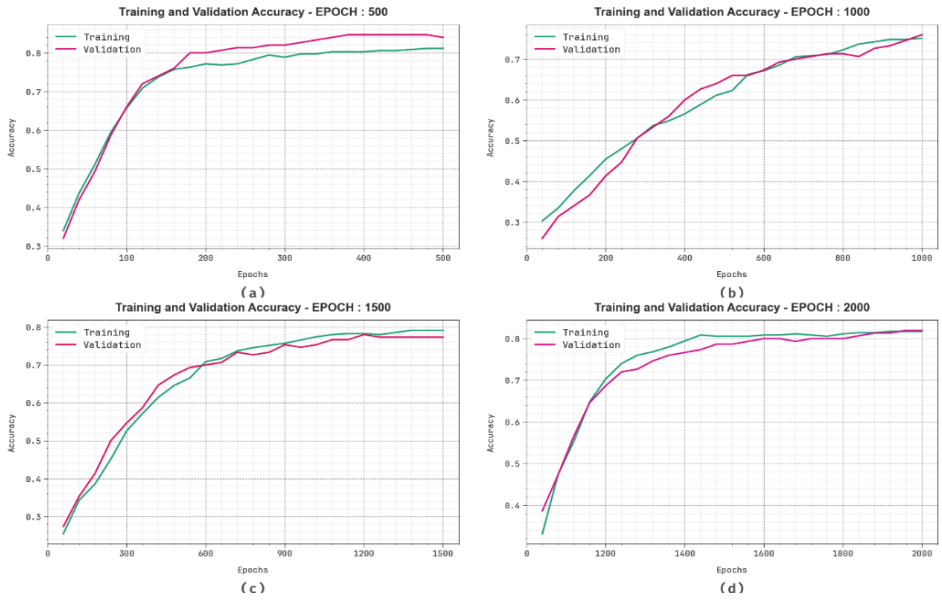

Figure 4. Accuracy curve of ECVDP-IBWOEL technique (a-d) Epochs 500-2000

The classifier outcomes of the ECVDP-IBWOEL algorithm are graphically displayed in Fig. 4 for training accuracy (TRA) and validation accuracy (VLA) curves. The result shows valuable study of the behavior of the ECVDP-IBWOEL system over different epochs, representing its generalization abilities and learning process. Notably, the figure specifies a constant development in the TRA and VLA with raising number of epochs. It assures the adaptable nature of the ECVDP-IBWOEL technique in the pattern detection model on both datasets. The rising trend in VALA defines the ability of the ECVDP-IBWOEL process to adapt to the TRA dataset and excel in providing correct classification of hidden dataset, presenting the strong generalisability.

Fig. 5 displays a complete analysis of the training loss (TRLA) and validation loss (VALL) outcomes of the ECVDP-IBWOEL model over various epochs. The progressive decline in TRLA emphasizes the ECVDP-IBWOEL technique increasing the weights and decreasing the classifier error on both datasets. The figure shows a clear insight of the ECVDP-IBWOEL model's relationship with the TRA dataset, which highlights its capability to capture patterns within both datasets. Notably, the ECVDP-IBWOEL system recurrently increases its parameters in diminishing the variances between the prediction and real TRA classes.

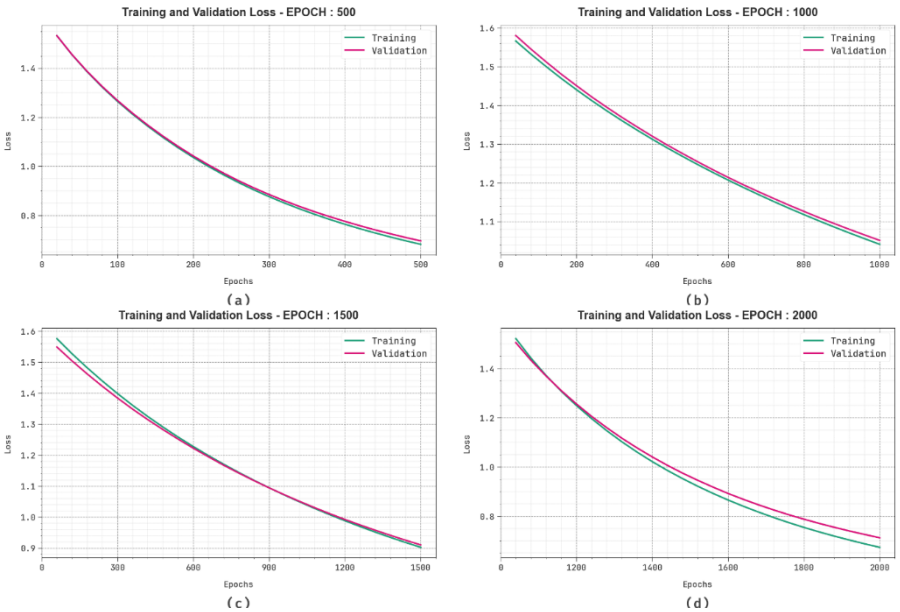

Figure 5. Loss curve of ECVDP-IBWOEL model (a-d) Epochs 500-2000

DOI: https://doi.org/10.54216/FPA.170213
Received: January 28, 2024 Revised: April 27, 2024 Accepted: September 26, 2024

Inspecting the PR curve, as presented in Fig. 6, the results certified that the ECVDP-IBWOEL method gradually achieves greater PR performance over below every class. It confirms the greater skills of the ECVDP-IBWOEL system in the classification of separate classes, presenting efficiency in the identification of classes.

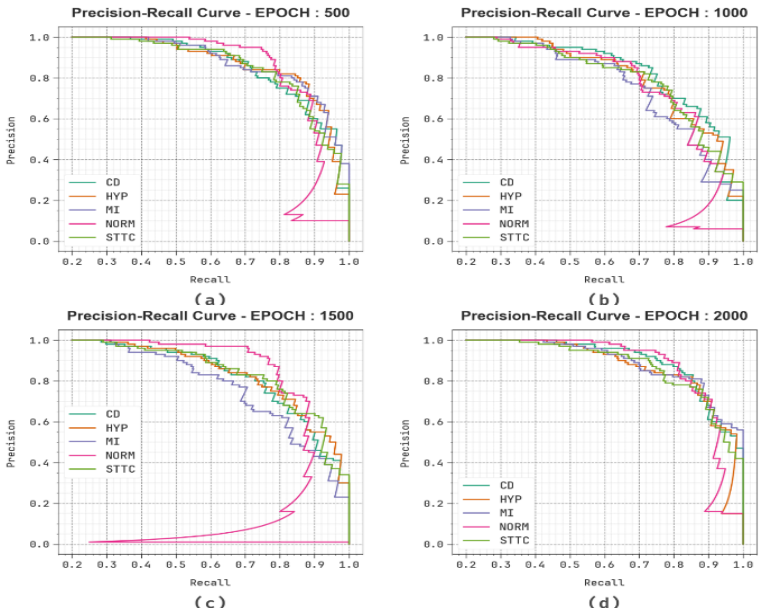

Figure 6. PR curve of ECVDP-IBWOEL technique (a-d) Epochs 500-2000

Also, in Fig. 7, ROC curves formed by the ECVDP-IBWOEL method outperformed the identification of dissimilar labels. It offers a thorough knowledge of the tradeoff amongst TPR and FRP over distinct detection threshold values and epochs. The figure emphasized the boosted classification results of the ECVDP-IBWOEL system under all classes, outlining the efficacy in addressing numerous identification problems.

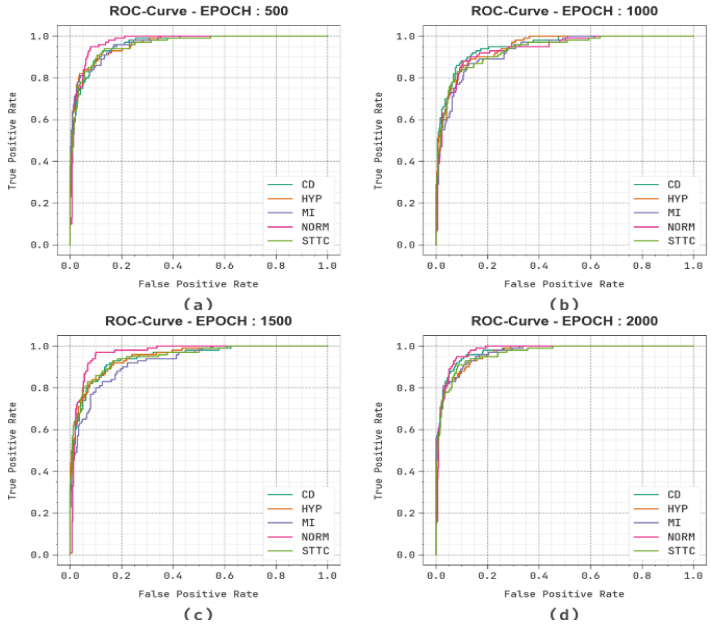

Figure 7. ROC curve of ECVDP-IBWOEL technique (a-d) Epochs 500-2000

In Table 2 and Fig. 8, the comparative study of the ECVDP-IBWOEL system is made with existing models [23]. The results imply that the 1-DCNN, LR, DT, and KNN models have shown poor performance with $accu_y$ values of 73.01%, 37.39%, 27.92%, and 66.90%, respectively. Meanwhile, DL-ECGA, GBT, and RF models have reported considerable performance with $accu_y$ values of 84.72%, 84.99%, and 79.84%, respectively.

DOI: https://doi.org/10.54216/FPA.170213
Received: January 28, 2024 Revised: April 27, 2024 Accepted: September 26, 2024

Table 2: $Accu_y$ outcome of ECVDP-IBWOEL technique with existing models

Methods	Accuracy (%)
ECVDP-IBWOEL	92.28
MROA-DLECGSC	88.98
DLECG-CVD	88.26
DL-ECGA	84.72
Gradient-Boosting Tree	84.99
Random Forest	79.84
1-DCNN Model	73.01
Logistic Regression	37.39
Decision Tree	27.92
K Neighbors Classifier	66.90

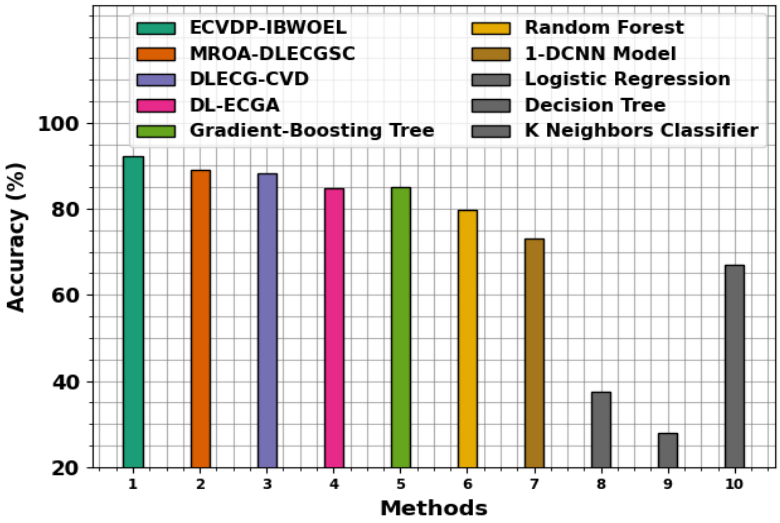

Figure 8. $Accu_y$ Outcome of ECVDP-IBWOEL technique with existing models

Furthermore, the MROA-DLECGSC model has resulted in reasonable outcomes with $accu_y$ of 88.98%. But the ECVDP-IBWOEL technique gains maximum performance with $accu_y$ of 92.28%. Therefore, the ECVDP-IBWOEL method can be exploited for enhanced prediction of CVD.

5. Conclusion

In this work, we have designed an ECVDP-IBWOEL technique via ECG signal analytics. The main intention of the ECVDP-IBWOEL approach is to forecast the incidence of CVD at the early stage using EEG signals. To accomplish that, the ECVDP-IBWOEL technique has three different kinds of methods such as data preprocessing, EL, and IBWO-based parameter tuning process. At the initial stage, the ECVDP-IBWOEL algorithm arises data preprocessing is performed to change the input data into a compatible format. Also, the ECVDP-IBWOEL method follows the EL process for CVD detection comprising three models namely LSTM, DBN, and SAE. Finally, the IBWO algorithm-based hyperparameter tuning process takes place which can boost the classifier results of the ensemble models. To certify the enhanced outcomes of the ECVDP-IBWOEL model, an extensive experimentation study is made. The experimental outcomes stated that the ECVDP-IBWOEL approach underlines promising performance in CVD prediction process.

Funding: "The author gratefully acknowledges technical support provided by the Faculty of Computing and Information Technology, King Abdulaziz University, Jeddah, Saudi Arabia."

Conflicts of Interest: "The authors declare no conflict of interest."

DOI: https://doi.org/10.54216/FPA.170213
Received: January 28, 2024 Revised: April 27, 2024 Accepted: September 26, 2024

References

[1] Mhamdi, L.; Dammak, O.; Cottin, F.; Dhaou, I.B. Artificial Intelligence for Cardiac Diseases Diagnosis and Prediction Using ECG Images on Embedded Systems. Biomedicines 2022, 10, 2013.

[2] Kumar, S.; Mallik, A.; Kumar, A.; Del Ser, J.; Yang, G. Fuzz-ClustNet: Coupled fuzzy clustering and deep neural networks for Arrhythmia detection from ECG signals. Comput. Biol. Med. 2023, 153, 106511.

[3] Agrawal, V.; Hazratifard, M.; Elmiligi, H.; Gebali, F. Electrocardiogram (ECG)-Based User Authentication Using Deep Learning Algorithms. Diagnostics 2023, 13, 439.

[4] Wang, P.; Lin, Z.; Yan, X.; Chen, Z.; Ding, M.; Song, Y.; Meng, L. A wearable ECG monitor for deep learning based real-time cardiovascular disease detection. arXiv 2022, arXiv:2201.10083.

[5] Sadiq, M.T.; Yu, X.; Yuan, Z. Exploiting dimensionality reduction and neural network techniques for the development of expert brain–computer interfaces. Expert Syst. Appl. 2021, 164, 114031.

[6] Maji, P.; Mondal, H.K.; Roy, A.P.; Poddar, S.; Mohanty, S.P. iKardo: An Intelligent ECG Device for Automatic Critical Beat Identification for Smart Healthcare. IEEE Trans. Consum. Electron. 2021, 67, 235–243.

[7] Rahaman, O.; Shamrat, F.M.J.M.; Kashem, M.A.; Akter, M.F.; Chakraborty, S.; Ahmed, M.; Mustary, S. Internet of things based electrocardiogram monitoring system using machine learning algorithm. Int. J. Electr. Comput. Eng. 2022, 12, 3739–3751.

[8] Aras, M.A.; Abreau, S.; Mills, H.; Radhakrishnan, L.; Klein, L.; Mantri, N.; Rubin, B.; Barrios, J.; Chehoud, C.; Kogan, E.; et al. Electrocardiogram Detection of Pulmonary Hypertension Using Deep Learning. J. Card. Fail. 2023, 29, 1017–1028.

[9] Ribeiro, H.D.M.; Arnold, A.; Howard, J.P.; Shun-Shin, M.J.; Zhang, Y.; Francis, D.P.; Lim, P.B.; Whinnett, Z.; Zolgharni, M. ECG-based real-time arrhythmia monitoring using quantized deep neural networks: A feasibility study. Comput. Biol. Med. 2022, 143, 105249.

[10] Khanna, A.; Selvaraj, P.; Gupta, D.; Sheikh, T.H.; Pareek, P.K.; Shankar, V. Internet of things and deep learning enabled healthcare disease diagnosis using biomedical electrocardiogram signals. Expert Syst. 2021, 40, e12864.

[11] Zhang, H., Zhang, P., Lin, F., Chao, L., Wang, Z., Ma, F. and Li, Q., 2024. Co-learning-assisted progressive dense fusion network for cardiovascular disease detection using ECG and PCG signals. Expert Systems with Applications, 238, p.122144.

[12] Karthik, S., Santhosh, M., Kavitha, M.S. and Paul, A.C., 2022. Automated Deep Learning Based Cardiovascular Disease Diagnosis Using ECG Signals. Computer Systems Science & Engineering, 42(1).

[13] Goud, P.S., Sastry, P.N. and Sekhar, P.C., 2023. A novel intelligent deep optimized framework for heart disease prediction and classification using ECG signals. Multimedia Tools and Applications, pp.1-17.

[14] Admass, W.S. and Bogale, G.A., 2024. Arrhythmia classification using ECG signal: A meta-heuristic improvement of optimal weighted feature integration and attention-based hybrid deep learning model. Biomedical Signal Processing and Control, 87, p.105565.

[15] Golande, A.L. and Pavankumar, T., 2023. Optical electrocardiogram based heart disease prediction using hybrid deep learning. Journal of Big Data, 10(1), p.139.

[16] Rai, H.M., Chatterjee, K. and Dashkevych, S., 2022. The prediction of cardiac abnormality and enhancement in minority class accuracy from imbalanced ECG signals using modified deep neural network models. Computers in Biology and Medicine, 150, p.106142.

[17] Khatar, Z., Bentaleb, D. and Bouattane, O., 2024. Advanced detection of cardiac arrhythmias using a three-stage CBD filter and a multi-scale approach in a combined deep learning model. Biomedical Signal Processing and Control, 88, p.105551.

[18] Tahmid, M.T., Kader, M.E., Mahmud, T. and Fattah, S.A., 2023. MD-CardioNet: A Multi-Dimensional Deep Neural Network for Cardiovascular Disease Diagnosis from Electrocardiogram. IEEE Journal of Biomedical and Health Informatics.

DOI: https://doi.org/10.54216/FPA.170213
Received: January 28, 2024 Revised: April 27, 2024 Accepted: September 26, 2024

[19] Kapoor, A., Negi, A., Marshall, L. and Chandra, R., 2023. Cyclone trajectory and intensity prediction with uncertainty quantification using variational recurrent neural networks. Environmental Modelling & Software, 162, p.105654.

[20] Zhang, C., Zhang, Y., Huang, Q. and Zhou, Y., 2023, March. Intelligent Fault Prognosis Method Based on Stacked Autoencoder and Continuous Deep Belief Network. In Actuators (Vol. 12, No. 3, p. 117). MDPI.

[21] Li, Y., Chen, Z., Hou, M. and Guo, T., 2024. Multi-objective optimization design of anti-roll torsion bar using improved beluga whale optimization algorithm. Railway Sciences, 3(1), pp.32-46.

[22] https://physionet.org/content/ptb-xl/1.0.3/

[23] Alluhaidan, A.S., Maashi, M., Arasi, M.A., Salama, A.S., Assiri, M. and Alneil, A.A., 2023. Mud Ring Optimization Algorithm with Deep Learning Model for Disease Diagnosis on ECG Monitoring System. Sensors, 23(15), p.6675.

DOI: https://doi.org/10.54216/FPA.170213
Received: January 28, 2024 Revised: April 27, 2024 Accepted: September 26, 2024